Electronic supporting information

Strong chiroptical properties from thin films of chiral imidazole derivatives allowing for easy detection of circularly polarized luminescence

Andrea Taddeucci†,[a] Caterina Campinoti†,[a] Francesca Sardelli,[a] Gennaro Pescitelli,[a] Lorenzo Di Bari,[a] Marco Lessi*,[a] Francesco Zinna*[a]

Dipartimento di Chimica e Chimica Industriale, Università di Pisa, via Moruzzi 13, 56124, Pisa, Italy.

Email: marco.lessi@unipi.it; francesco.zinna@unipi.it

† These authors contributed equally.

Synthetic procedures

General Information

Melting points were recorded on a hot-stage microscope (Reichert Thermovar). Precoated silica gel PET foils (Sigma-Aldrich) were used for TLC analyses. GLC-FID analyses were performed on a Dani GC 1000 chromatograph equipped with a PTV injector, using an Agilent J&W DB-1 column (15 m x 0.25 mm x 0.25 μm) and recorded with a Dani DDS 1000 data station and a Shimadzu Nexis GC-2030 using an Agilent J&W DB-5 column (30 m x 0.25 mm x 0.25 μm). GLC-MS analyses were recorded with an Agilent 6890N gas chromatograph interfaced with an Agilent MS5973 mass detector, using an Agilent J&W DB-5ms (30 m x 0.25 mm x 0.25 μm) column. LC-MS-DAD analyses were performed on an Acquity UPLC Water instrument (Phase A 95/5 H_2O / ACN + 0.1% Formic Acid, Phase B 5/95 H2O / ACN + 0.1% Formic Acid; Acquity UPLC 2.1x100 mm column, BEH C18, 1.7 μm; Flow 0.5 mL / min) coupled with an Acquity QDa Water mass spectrometer (Probe temperature: 600 °C; ESI capillary voltage 1.5 kV; Cone voltage 15 V; Mass range 60-1000 Da) and a PDA eλ Detector (wavelenght range 200-800 nm). Purifications by flash chromatography were performed using Merck 60 silica gel. ^{1}H-NMR and ^{13}C-NMR spectra were recorded with a JEOL ECZS 400 MHz and JEOL ECZR 500 MHz instruments. The chemical shifts were referred to the residual solvent signal. The following notation was used in order to report NMR spectra: s = singlet, bs = broad singlet, d = doublet, dd = double doublet, t = triplet, dt = double triplet, q = quadruplet, m = multiplet. 1-methyl-1H-imidazole and TMEDA were distilled under reduced pressure over CaH_2, piperidine and Et_3N were distilled at atmospheric pressure, NBS was purified by recrystallization. All the other commercially available reagents and solvents were used as received. GLC or UPLC analysis showed that compounds **1**-**4** had chemical purity higher than 98%.

Procedures

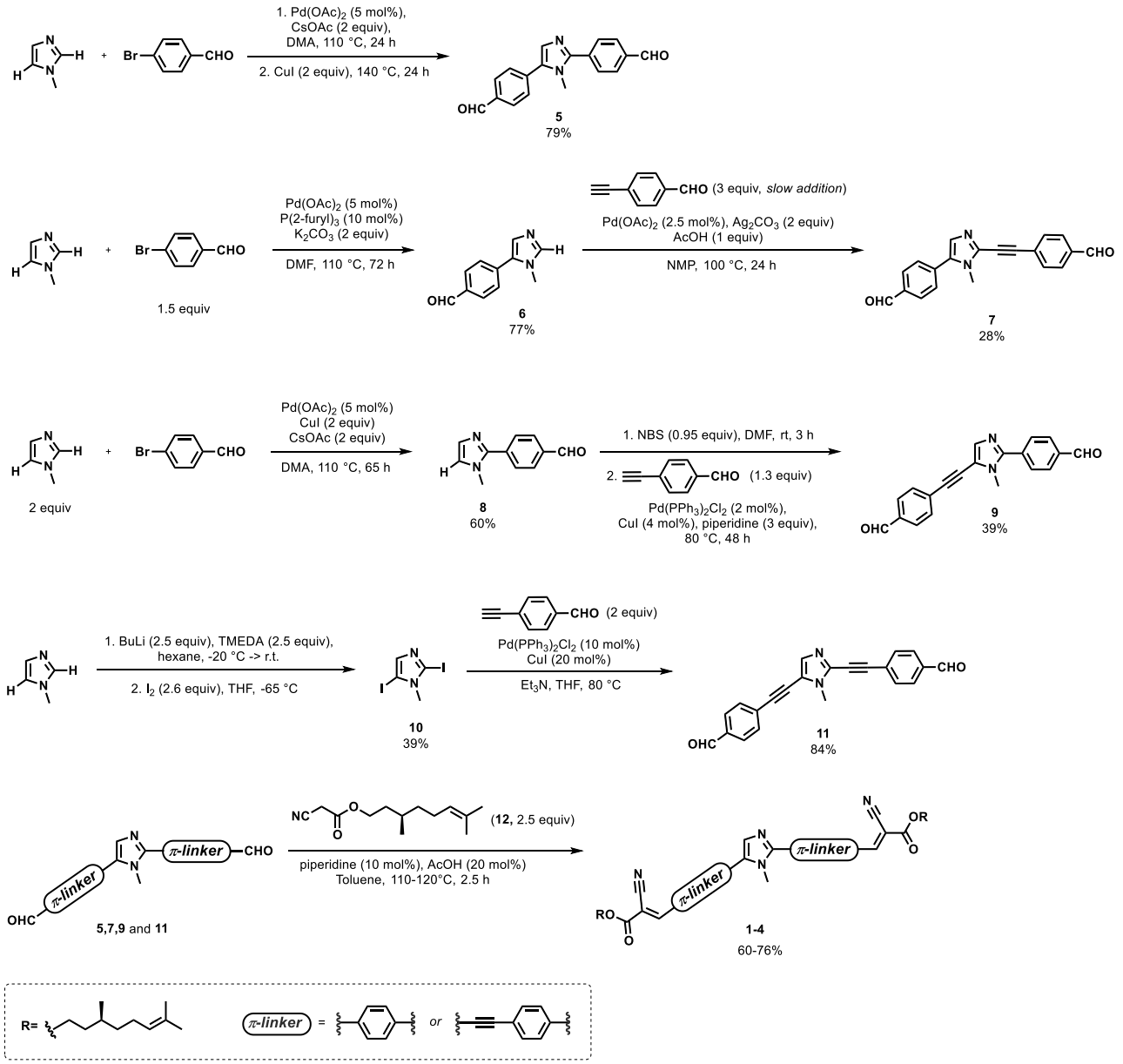

Scheme S1

Synthesis of 4,4'-(1-methyl-1H-imidazole-2,5-diyl)dibenzaldehyde (5)

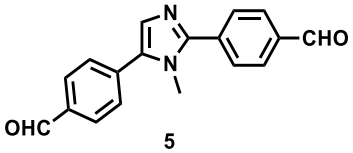

In a flame-dried two-neck flask 1-methyl-1H-imidazole (5 mmol, 380 µL) and 4-bromobenzaldehyde (3 equiv., 2.78 g), $Pd(OAc)_2$ (5 mol%, 56 mg) and CsOAc (2 equiv., 1.92 g) were loaded. After three vacuum-argon cycles, anhydrous DMA (25 mL). The reaction mixture was stirred at 110 °C for 24 h and monitored with TLC, GC-FID and GC-MS analysis. Then, CuI (2.0 equiv., 1.90 g) was added and the temperature was increased to 140 °C; the resulting mixture was stirred for other 24 h.

The reaction mixture was then cooled to room temperature and diluted with DCM. Saturated aqueous NH_4Cl solution and few milliliters of NH_4OH 30% were added to the reaction mixture. The resulting mixture was stirred for 30 min, then the organic layer was washed with saturated aqueous NH_4Cl solution and NH_4OH 30% until decoloration of aqueous phase. The aqueous layer was back-washed twice with organic solvent. Finally,

the collected organic phases were washed with brine, dried with anhydrous Na_2SO_4 and concentrated under reduced pressure. The reaction crude was purified by flash chromatography on silica gel with a mixture of DCM and AcOEt (8:2) as eluent to give **5** as a yellow solid (1.14 g, 79%).
The spectral properties of this compound are in agreement with those previously reported.[S1]
mp 164-165 °C.
^{1}H NMR (400 MHz, $CDCl_3$) δ (ppm): 10.08 (s, 1H), 10.06 (s, 1H), 8.02 (m, 4H), 8.00 (m, 2H), 7.65 (m, 2H), 7.39 (s, 1H), 3.79 (s, 3H).
^{13}C NMR (500 MHz, $CDCl_3$) δ (ppm): 191.7, 191.5, 136.2, 135.9, 135.6, 135.6, 130.4, 130.0, 129.9, 129.3, 128.9, 128.7, 34.5.
EI-MS: m/z 290 (100%), 261 (8), 158 (11), 130 (9), 89 (8).

Synthesis of 4-(1-methyl-1H-imidazol-5-yl)benzaldehyde (6)

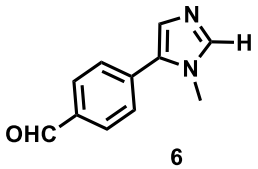

6

In a flame-dried two-neck flask 4-bromobenzaldehyde (1.5 equiv, 1.388 g), $Pd(OAc)_2$ (5 mol%, 56 mg), P(2-furyl)$_3$ (10 mol%, 116 mg), K_2CO_3 (2 equiv., 1.382 g) were added; after three vacuum/argon cycles, anhydrous DMF (25 mL) and 1-methyl-1H-imidazole (5 mmol, 396 µL) were added too. The reaction mixture was stirred at 110 °C for 72 h. The reaction mixture was then cooled at room temperature, diluted with a mixture of DCM and AcOEt (1:1, 100 mL), filtered through a plug of celite and concentrated under reduced pressure. The residue was purified by flash chromatography on silica gel with a mixture of DCM + 6% MeOH as eluent to give **6** as a yellow solid (715 mg, 77%).
The spectral properties of this compound are in agreement with those previously reported.[S2]
mp 89-90 °C
^{1}H NMR (400 MHz, $CDCl_3$) δ 10.04 (s, 1H), 8.00 – 7.92 (m, 2H), 7.61 – 7.55 (m, 3H), 7.24 (s, 1H), 3.75 (s, 3H).
^{13}C NMR (500 MHz, $CDCl_3$) δ 191.7, 140.5, 135.9, 135.4, 132.4, 130.3, 129.9, 128.4, 33.1.
EI-MS: m/z 187 (12%), 186 (100), 185 (85), 157 (6), 130 (13).

Synthesis of 4-((5-(4-formylphenyl)-1-methyl-1H-imidazol-2-yl)ethynyl)benzaldehyde (7)

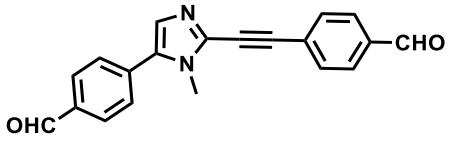

7

In a two-neck flask 4-(1-methyl-1H-imidazol-5-yl)benzaldehyde **6** (1 mmol, 190 mg), $Pd(OAc)_2$ (2.5 mol%, 5.6 mg), Ag_2CO_3 (2 equiv., 552 mg), AcOH (1 equiv., 57.2 µL) and NMP (2 mL) were added. A solution of 4-etynylbenzaldehyde (3 equiv., 390 mg) in NMP (2 mL) over 2 h. The reaction mixture was stirred at 100 °C for 3.5h. The reaction mixture was then cooled at room temperature, diluted with a mixture of DCM and AcOEt (1:1, 50 mL), filtered through a plug of celite and concentrated under reduced pressure. The residue was purified by flash chromatography on silica gel with a mixture of DCM and AcOEt (8:2) as eluent to give **7** as a yellow solid (44 mg, 28%).
mp 132-134 °C
^{1}H NMR (400 MHz, $CDCl_3$) δ 10.07 (s, 1H), 10.04 (s, 1H), 8.04 – 7.95 (m, 2H), 7.94 – 7.87 (m, 2H), 7.79 – 7.71 (m, 2H), 7.68 – 7.57 (m, 2H), 7.33 (s, 1H), 3.88 (s, 3H).
^{13}C NMR (500 MHz, $CDCl_3$) δ 191.5, 191.4, 136.3, 135.8, 135.2, 132.3, 130.7, 130.4, 129.8, 128.6, 127.9, 93.1, 82.5, 33.1.
ESI-MS: m/z 315 ($[M–H]^+$)

Synthesis of 4-(1-methyl-1H-imidazol-2-yl)benzaldehyde (8)

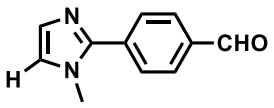

8

In a flame-dried two-neck flask 4-bromobenzaldehyde (5 mmol, 925 mg), $Pd(OAc)_2$ (5 mol%, 56 mg), CuI (2 equiv., 1.9 g), CsOAc (2 equiv., 1.92 g) were added; after three vacuum/argon cycles, anhydrous DMA (30 mL) and 1-methyl-1*H*-imidazole (5 mmol, 398 µL) were added too. The reaction mixture was stirred at 110 °C for 65h. The reaction mixture was then cooled at room temperature, diluted with AcOEt (200 mL), then saturated aqueous NH_4Cl (100 mL) and NH_3 (4 mL) were added. The resulting mixture was stirred for 30 minutes and extracted with AcOEt (3x50 mL). The organic extracts were washed with saturated aqueous NH_4Cl (50 mL) and brine (50 mL), dried over Na_2SO_4, filtered and concentrated under reduced pressure. The residue was purified by flash chromatography on silica gel with a mixture of DCM and MeOH (9:1) as eluent to give **8** as a yellow oil (555 mg, 60%).
The spectral properties of this compound are in agreement with those previously reported.[S3]
^{1}H NMR (500 MHz, $CDCl_3$) δ 10.05 (s, 1H), 7.96 (d, J = 7.7 Hz, 2H), 7.84 (d, J = 8.4 Hz, 2H), 7.17 (s, 1H), 7.02 (s, 1H), 3.81 (s, 3H).
^{13}C NMR (500 MHz, $CDCl_3$) δ = 191.7, 146.3, 136.2, 135.9, 129.1, 128.9, 128.8, 123.3, 34.8.
EI-MS: m/z 187 (12%), 186 (100), 185 (93), 157 (23), 156 (20).

Synthesis of 4-((2-(4-formylphenyl)-1-methyl-1H-imidazol-5-yl)ethynyl)benzaldehyde (9)

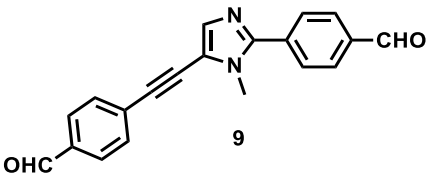

9

In a flame-dried two-neck flask NBS (0.95 equiv., 244 mg) was added; after three vacuum/argon cycles, anhydrous DMF (7.5 mL) and 4-(1-methyl-1H-imidazol-2-yl)benzaldehyde **8** (1.5 mmol, 277 mg) were added too. The reaction mixture was stirred at room temperature for 3h and monitored through GC-FID analysis. Then 4-ehtynylbenzaldehyde (1.1 equiv., 215 mg), $PdCl_2(PPh_3)_2$ (2 mol%, 21 mg), CuI (4 mol%, 12 mg) and piperidine (3 equiv., 443 µL) were added in one portion and the resulting mixture was stirred at 80 °C for 26 h. The reaction mixture was then cooled at room temperature, diluted with DCM (100 mL), then saturated aqueous NH_4Cl (100 mL) was added. The resulting mixture was stirred for 30 minutes and extracted with DCM (3x25 mL). The organic extracts were washed with water (2x25 mL) and brine (25 mL), dried over Na_2SO_4, filtered and concentrated under reduced pressure. The residue was purified by flash chromatography on silica gel with a mixture of petroleum ether and acetone (65:35) as eluent to give **9** as a yellow solid (179 mg, 38%).
mp 102-103 °C
^{1}H NMR (400 MHz, $CDCl_3$) δ 10.10 (s, 1H), 10.04 (s, 1H), 8.03 (d, J = 8.6 Hz, 2H), 7.91 (m, 4H), 7.69 (d, J = 8.2 Hz, 2H), 7.58 (s, 1H), 3.91 (s, 3H).
^{13}C NMR (500 MHz, $CDCl_3$) δ 191.7, 191.4, 177.4, 147.7, 136.4, 135.8, 135.7, 135.6, 131.8, 130.1, 129.8, 129.2, 129.1, 128.6, 118.5, 97.0, 81.6, 33.4, 29.8, 29.7.
ESI-MS: m/z 315 ($[M–H]^+$)

Synthesis of 2,5-diiodo-1-methyl-1H-imidazole (10)

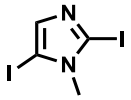

10

In a flame-dried three-neck flask containing anhydrous hexane (5.2 mL), n-BuLi (1.6 M, 2.5 equiv., 7.8 mL) and TMEDA (2.55 equiv., 1.9 mL) were added at -20 °C. Then 1-methyl-1*H*-imidazole (5 mmol, 399 µL) was added dropwise. The resulting heterogeneous mixture was allowed to warm at room temperature over 1 h. Anhydrous THF was added (4.7 mL) and the mixture was cooled to -65 °C. A solution of I_2 (2.6 equiv., 3.3 g) in anhydrous THF (17 mL) was added dropwise over 80 min. The mixture was then allowed to warm to room temperature over the night and quenched with AcOEt (5 mL) and water (5 mL). DCM (60 mL) and an aqueous solution of $Na_2S_2O_3$ (10%, 30 mL) were added and the resulting organic extracts were washed with $Na_2S_2O_3$ (10%, 3x25 mL) and brine (25 mL), dried over Na_2SO_4, filtered and concentrated under reduced pressure. The residue was purified by flash chromatography on silica gel with a mixture of DCM and AcOEt (9:1) as eluent to give **10** as a white solid (525 mg, 37%).
The spectral properties of this compound are in agreement with those previously reported.[S4]
mp 153-154 °C
^{1}H NMR (400 MHz, $CDCl_3$) δ 7.17 (s, 1H), 3.65 (s, 3H).
EI-MS: m/z 228 (8%), 138 (8), 123 (22), 95 (36), 81 (30), 69 (100).

Synthesis of 4,4'-((1-methyl-1H-imidazole-2,5-diyl)bis(ethyne-2,1-diyl))dibenzaldehyde (11)

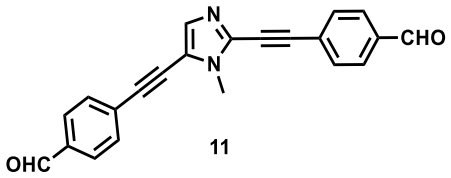

11

In a flame-dried two-neck flask 2,5-diiodo-1-methyl-1H-imidazole **10** (0.5 mmol, 166 mg), $Pd(PPh_3)_2Cl_2$ (7.3 mol%, 25.6 mg), CuI (17 mol%, 16.2 mg), PPh_3 (0.87 equiv., 111 mg) were added; after three vacuum/argon cycles, anhydrous THF (5 mL) and Et_3N (10 mL) were added too. The reaction mixture was stirred at reflux for 15 h. The reaction mixture was then cooled at room temperature, reduced concentrated under reduced pressure, diluted with AcOEt (60 mL) and extracted with brine (60 mL). The organic extracts were washed with brine (2x30 mL) and a saturated aqueous solution of NH_4Cl (40 mL), dried over Na_2SO_4, filtered and concentrated under reduced pressure. The residue was purified by flash chromatography on silica gel with a mixture of DCM + 5% acetone as eluent to give **11** as a yellow solid (142 mg, 84%).
mp 177-179 °C
^{1}H NMR (400 MHz, $CDCl_3$) δ 10.05 (s, 1H), 10.04 (s,1H), 7.91 (m, 2H), 7.89 (m, 2H) 7.75 (m, 2H), 7.67 (m, 2H), 7.47 (s, 1H), 3.88 (s, 3H).
^{13}C NMR (500 MHz, $CDCl_3$) δ 191.4, 136.0, 135.9, 132.4, 131.9, 129.8, 129.8, 127.6, 96.5, 63.6, 53.3, 46.0, 32.4, 29.8, 8.8, 8.4.
ESI-MS: m/z 339 ($[M–H]^+$)

Synthesis of (S)-3,7-dimethyloct-6-en-1-yl 2-cyanoacetate (12)

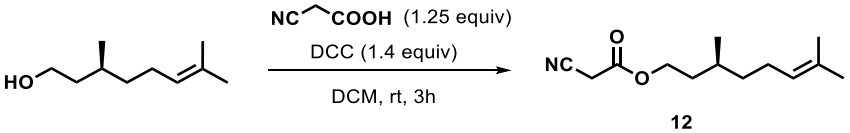

12
95%

In a flame-dried two-neck flask cyanoacetic acid (1.25 equiv, 479 mg), anhydrous DCM (12 mL) and (S)-citronellol (4.5 mmol, 832 µL) were added; after cooling the mixture to 0 °C, DCC (1.4 equiv., 1.3 g) was added too. The reaction mixture was stirred at room temperature for 3 h. The reaction mixture was diluted with DCM (50 mL), filtered through a plug of celite and concentrated under reduced pressure. The residue was purified by flash chromatography on silica gel with a mixture of DCM and petroleum ether (7:3) as eluent to give **12** as a colorless oil (953 mg, 95%).

^{1}H NMR (400 MHz, $CDCl_3$) δ (ppm): 5.07 (m, 1H), 4.24 (m, 2H), 3.44 (s, 2H), 1.97 (m, 2H), 1.72 (m, 1H), 1.63 (d, 6H), 1.51 (m, 2H), 1.32 (m, 1H), 1.21 (m, 1H), 0.91 (d, 3H).
^{13}C NMR (500 MHz, $CDCl_3$) δ (ppm): 163.2, 113.2, 65.5, 36.9, 35.1, 29.3, 25.7, 25.3, 24.8, 19.5, 19.6, 17.7.
EI-MS: m/z 223 (8%), 138 (8), 123 (22), 95 (36), 81 (30), 69 (100)

General Procedure for the Knoevenagel Reaction of 1-4

In a two-neck flask connected to a Dean Stark Apparatus and to a refrigerant, the appropriate dialdehyde (1 equiv.) and cyanoacetic ester **12** (2.5 equiv.) were added, together with toluene (4 mL/mol). The mixture was stirred for few minutes until complete dissolution of the solid. Finally, piperidine (0.01 equiv.) and AcOH (0.02 equiv.) were added, and the resulting mixture was stirred for 2.5 hunder reflux (T=110-120 °C), monitoring through TLC analyses. Reaction mixture was then allowed to cool to room temperature, diluted with DCM and extracted several times with water. The aqueous phase was then washed with DCM until complete decolouration. Finally, the organic phase was washed with brine, dried with Na_2SO_4 overnight and concentrated under reduced pressure. The crude was then purified by flash chromatography.

Bis((S)-3,7-dimethyloct-6-en-1-yl)-3,3'-((1-methyl-1H-imidazole-2,5-diyl)bis(4,1-phenylene))(2,2')-bis(2-cyanoacrylate) (1)

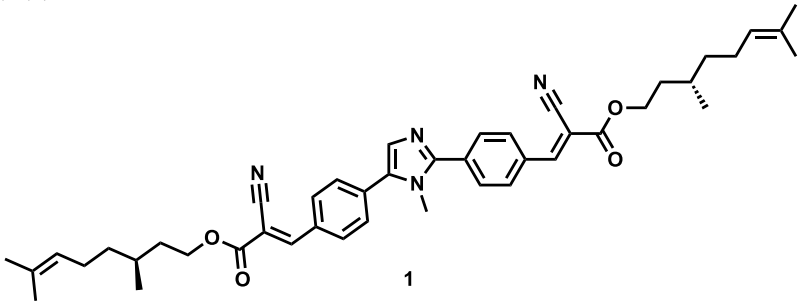

1

The crude reaction product obtained from the reaction of the dialdehyde **5** (0.5 mmol, 145 mg) with (S)-3,7-dimethyloct-6-en-1-yl-2-cyanoacetate **12** (1.25 mmol, 279 mg) was purified by flash chromatography on silica gel with a mixture of DCM and AcOEt (9:1) as eluent to give **1** as a bright yellow solid (250 mg, 75%).
mp 122-125 °C
Elemental Anal. Found: C, 75.49; H, 7.45; N, 7.93. Calc. for $C_{44}H_{52}N_4O_4$: C, 75.40; H, 7.48; N, 7.99.
^{1}H NMR (400 MHz, $CDCl_3$) δ (ppm): 8.27 (m, 2H), 8.12 (m, 4H), 7.89 (m, 2H), 7.64 (m, 2H), 7.40 (s, 1H), 5.10 (m, 2H), 4.37 (m, 4H), 3.82 (s, 3H), 2.01 (m, 4H), 1.81 (m, 2H), 1.64 (d, 12H), 1.58 (m, 4H), 1.38 (m, 2H), 1.26 (m, 2H), 0.97 (d, 6H).
^{13}C NMR (500 MHz, $CDCl_3$) δ (ppm): 162.5, 153.8, 149.4, 135.5, 134.7, 134.4, 131.8, 131.6, 131.5, 131.0, 130.2, 129.4, 128.7, 124.5, 115.57, 115.50, 103.8, 103.4, 65.5, 37.0, 35.4, 34.7, 29.6, 25.8, 25.5, 19.5, 17.8.
ESI-MS: m/z 702 ($[M–H]^+$)

(S)-3,7-dimethyloct-6-en-1-yl-2-cyano-3-(4-((5-(4-(2-cyano-3-(((S)-3,7-dimethyloct-6-en-1-yl)oxy)-3-oxoprop-1-en-1-yl)phenyl)-1-methyl-1H-imidazol-2-yl)ethynyl)phenyl)acrylate (2)

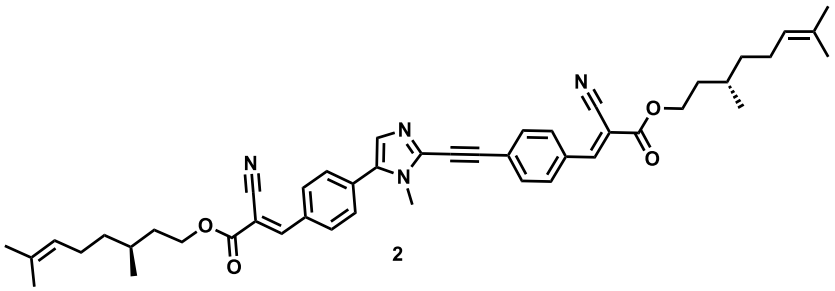

2

The crude reaction product obtained from the reaction of the dialdehyde **7** (0.4 mmol, 126 mg) with (S)-3,7-dimethyloct-6-en-1-yl 2-cyanoacetate **12** (1 mmol, 223 mg) was purified by flash chromatography on silica gel with a mixture of DCM + 5% AcOEt as eluent to give **2** as a bright yellow solid (211 mg, 73%).
mp 111-112 °C
Elemental Anal. Found: C, 76.30; H, 7.25; N, 7.69. Calc. for $C_{46}H_{52}N_4O_4$: C, 76.21; H, 7.23; N, 7.73.

^{1}H NMR (400 MHz, $CDCl_3$) δ 8.26 (s, 1H), 8.22 (s, 1H), 8.10 (d, J = 8.5 Hz, 2H), 8.01 (d, J = 8.6 Hz, 2H), 7.70 (d, J = 8.5 Hz, 2H), 7.60 (s, 2H), 7.35 (s, 1H), 5.15 – 5.04 (m, 2H), 4.47 – 4.30 (m, 4H), 3.89 (s, 3H), 2.02 (m, 4H), 1.83 (m, 2H), 1.65 (m, 16H), 1.39 (m, 2H), 1.24 (mp, 2H), 0.97 (dd, J = 6.5, 2.3 Hz, 6H).
^{13}C NMR (500 MHz, $CDCl_3$) δ 162.5, 162.4, 153.8, 153.5, 147.6, 134.3, 133.9, 133.8, 132.4, 131.9, 131.8, 131.6, 131.5, 131.1, 130.9, 128.6, 126.6, 124.5, 115.5, 115.4, 104.0, 103.5, 93.3, 82.8, 65.6, 37.0, 35.3, 33.2, 29.5, 25.8, 25.4, 19.5, 17.8.
ESI-MS: m/z 726 ([M–H]$^+$)

(S)-3,7-dimethyloct-6-en-1-yl-2-cyano-3-(4-((2-(4-(2-cyano-3-(((S)-3,7-dimethyloct-6-en-1-yl)oxy)-3-oxoprop-1-en-1-yl)phenyl)-1-methyl-1H-imidazol-5-yl)ethynyl)phenyl)acrylate (3)

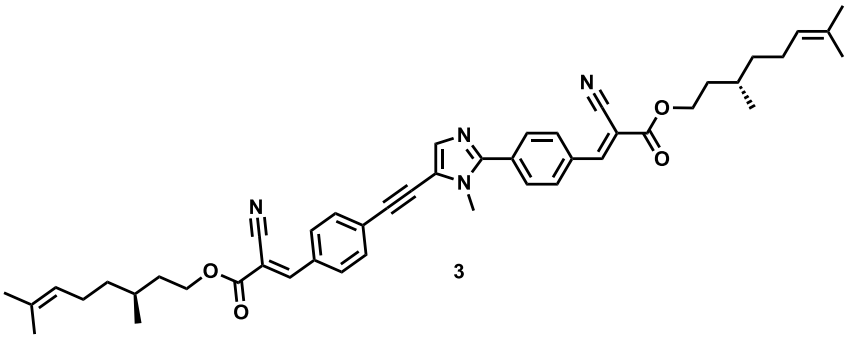

The crude reaction product obtained from the reaction of the dialdehyde **9** (0.5 mmol, 157 mg) with (S)-3,7-dimethyloct-6-en-1-yl 2-cyanoacetate **12** (1.25 mmol, 279 mg) was purified by flash chromatography on silica gel with a mixture of petroleum ether and AcOEt (7:3) as eluent to give **3** as a bright orange solid (217.4 mg, 60%).
mp 116-118 °C
Elemental Anal. Found: C, 76.39; H, 7.21; N, 7.65. Calc. for $C_{46}H_{52}N_4O_4$: C, 76.21; H, 7.23; N, 7.73.
^{1}H NMR (500 MHz, $CDCl_3$) δ 8.27 (s, 1H), 8.22 (s, 1H), 8.11 (d, J = 8.6 Hz, 2H), 8.01 (d, J = 8.3 Hz, 2H), 7.87 (d, J = 8.6 Hz, 2H), 7.63 (d, J = 8.4 Hz, 2H), 7.56 (s, 1H), 5.10 (ddq, J = 8.6, 5.7, 1.5 Hz, 2H), 4.37 (tdd, J = 6.8, 5.8, 4.2 Hz, 4H), 3.9 (s, 3H), 2.01 (m, 4H), 1.81 (m, 2H), 1.65 (m, 16H), 1.39 (m, 2H), 1.24 (m, 2H), 0.97 (dd, J = 6.5, 2.2 Hz, 6H).
^{13}C NMR (500 MHz, $CDCl_3$) δ 162.5, 162.5, 153.8, 153.6, 147.6, 135.9, 134.3, 131.9, 131.8, 131.6, 131.5, 131.4, 131.2, 129.1, 127.4, 124.5, 118.6, 115.5, 103.9, 103.6, 97.3, 81.9, 65.5, 37.0, 35.3, 33.5, 29.5, 25.8, 25.4, 19.5, 17.8.
ESI-MS: m/z 726 ([M–H]$^+$)

Bis((S)-3,7-dimethyloct-6-en-1-yl)-3,3'-(((1-methyl-1H-imidazole-2,5-diyl)bis(ethyne-2,1-diyl))bis(4,1-phenylene))-bis(2-cyanoacrylate) (4)

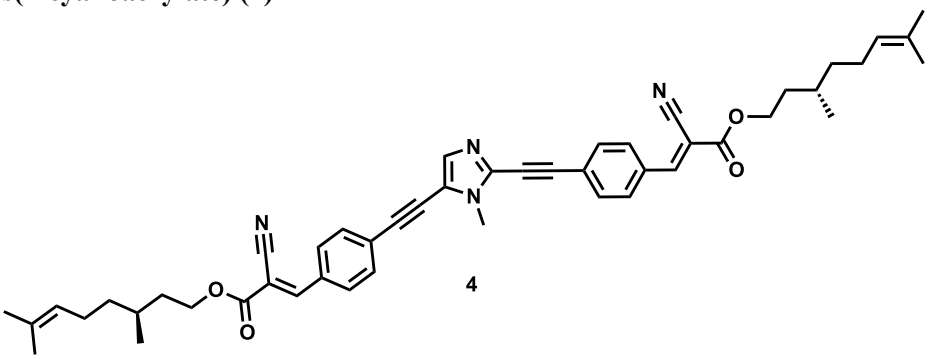

The crude reaction product obtained from the reaction of the dialdehyde **11** (0.35 mmol, 119 mg) with (S)-3,7-dimethyloct-6-en-1-yl 2-cyanoacetate **12** (0.88 mmol, 196 mg) was purified by flash chromatography on silica gel with a mixture of petroleum ether and AcOEt (7:3) as eluent to give **4** as a bright orange solid (197.1 mg, 75%).
mp 97-98 °C
Elemental Anal. Found: C, 77.01; H, 7.01; N, 7.52. Calc. for $C_{48}H_{52}N_4O_4$: C, 76.98; H, 7.00; N, 7.48.

^{1}H NMR (400 MHz, $CDCl_3$) δ 8.22 (s, 2H), 8.05 – 7.98 (m, 4H), 7.70 (d, J = 8.4 Hz, 2H), 7.66 – 7.60 (m, 2H), 7.48 (s, 1H), 5.10 (tt, J = 7.1, 1.4 Hz, 1H), 4.45 – 4.27 (m, 3H), 3.88 (s, 3H), 2.01 (m, 4H), 1.81 (m, 2H), 1.64 (m, 16H), 1.39 (m, 2H), 1.24 (mp, 2H), 0.98 (s, 3H), 0.96 (s, 3H).
^{13}C NMR (500 MHz, $CDCl_3$) δ 162.5, 162.4, 153.5, 153.4, 136.2, 132.8, 132.5, 132.0, 131.9, 131.6, 131.5, 131.2, 131.1, 127.1, 126.3, 124.5, 117.2, 115.4, 115.3, 104.1, 103.7, 96.8, 93.0, 82.2, 81.2, 65.6, 65.5, 37.0, 35.3, 32.4, 29.8, 29.5, 25.8, 25.4, 19.5, 17.8.
ESI-MS: m/z 750 ($[M-H]^+$)

Films preparation

All films were deposited on optical microscopy glass (1 mm thick and 2.5x2.5 mm in area). Thin film of **1** was prepared by spin coating 100 µL of a $5x10^{-3}$ M DCM solution of the compound at 55 rpm for 10 sec, with an acceleration rate of 55 rpm/sec.. Thin films of **2**-**4** were prepared by spin coating 150 µL of a $2x10^{-2}$ DCM solution of the compound at 1000 rpm for 30 sec, with an acceleration rate of 1000 rpm/sec. After deposition, all films were solvent annealed for 20 minutes in a DCM-saturated chamber.

Spectroscopy

General information

Solution absorption spectra were recorded with a Jasco V-650 spectrophotometer. Thin film absorption and ECD spectra were recorded with a Jasco J-1500 spectropolarimeter. Thin film fluorescence and CPL spectra were recorded with a home-built CPL spectrofluoropolarimeter,[S5] under 365 nm irradiation, using a 0° geometry between illumination and detection.[S6]
It is worth emphasizing that chiroptical measurements have been carried out as a function of sample's orientation for every thin film material. This allowed us to ascertain the absence of signal contributions arising from linear anisotropies of the sample (i.e. LDLB effect) or linear strain retained from the spectropolarimeter polarization-modulation system.[S7]

Characterization of the materials

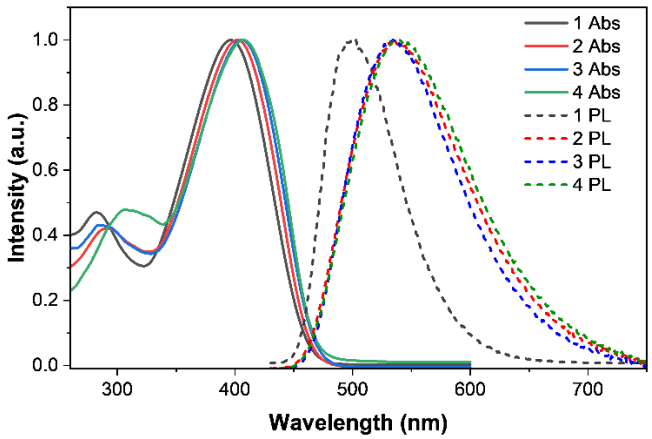

Fig S1. Normalized absorption and photoluminescence (PL) spectra of compounds **1**-**4** in chloroform solution.

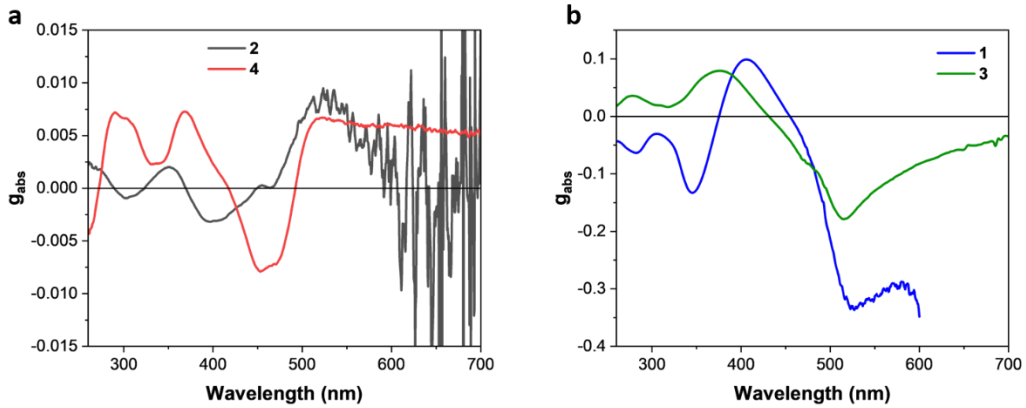

Fig. S2. Thin film g_{abs} spectra of couple of compounds (a) **2**/**4** and (b) **1**/**3**.

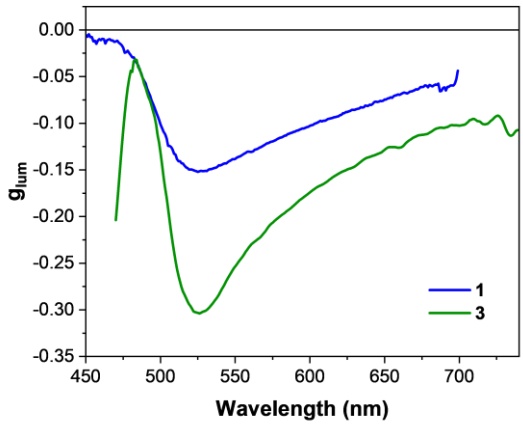

Fig. S3. Thin film g_{lum} spectra of compounds **1**/**3**.

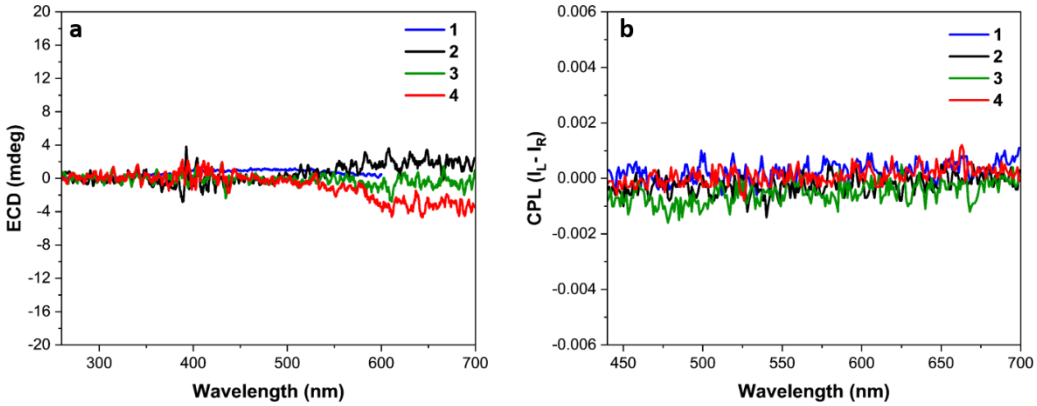

Fig. S4. (a) ECD and (b) CPL spectra of 3.5×10^{-5} M dichloromethane solutions of compounds **1-4**.

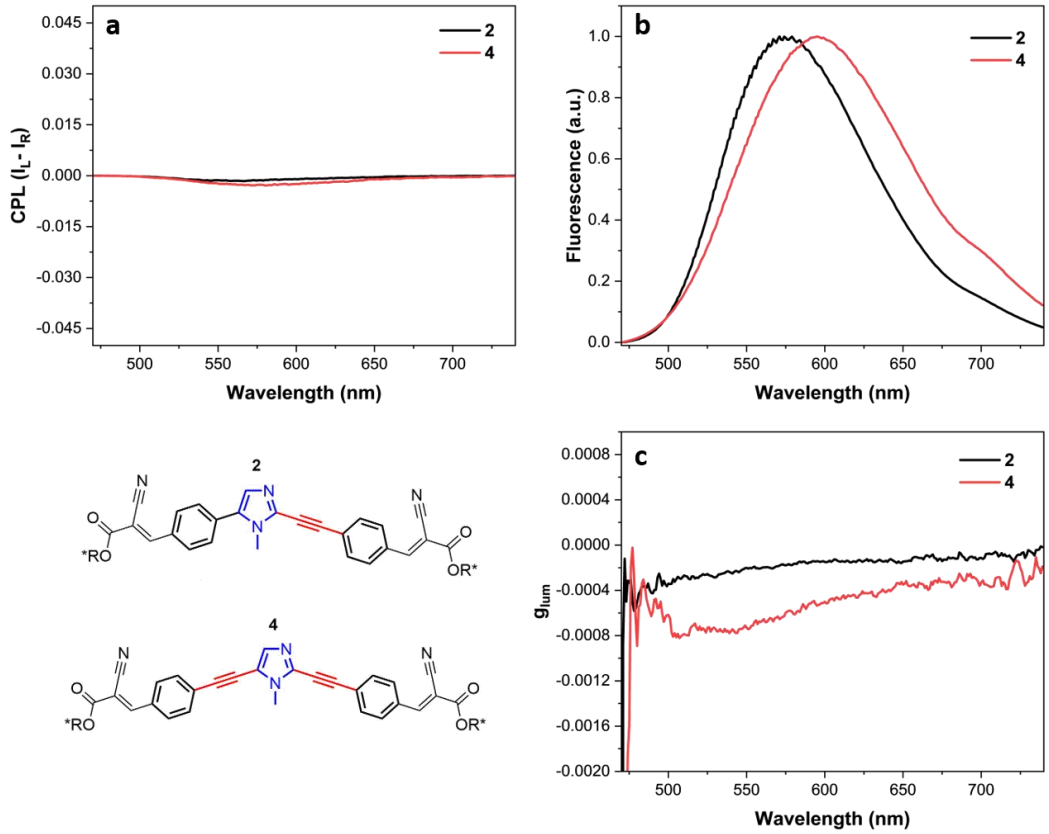

Fig. S5. (a) CPL, (b) fluorescence and (c) g_{lum} spectra of thin films made by compounds **2**/**4**.

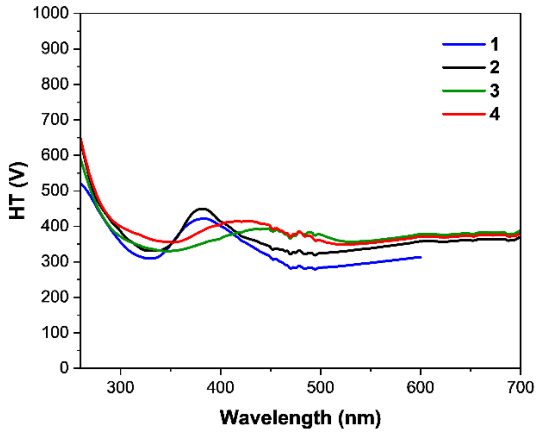

Fig. S6. HT relative to ECD measurements of thin films made by compounds **1-4**, before blank (glass substrate) subtraction.

Variable thickness films

By varying the concentration of the spin-coated solution, films of compound 3 with various thickness were prepared with respect to the original film (film C, thickness 200 nm): A, 50% of C thickness; B, 75%; D, 200%.

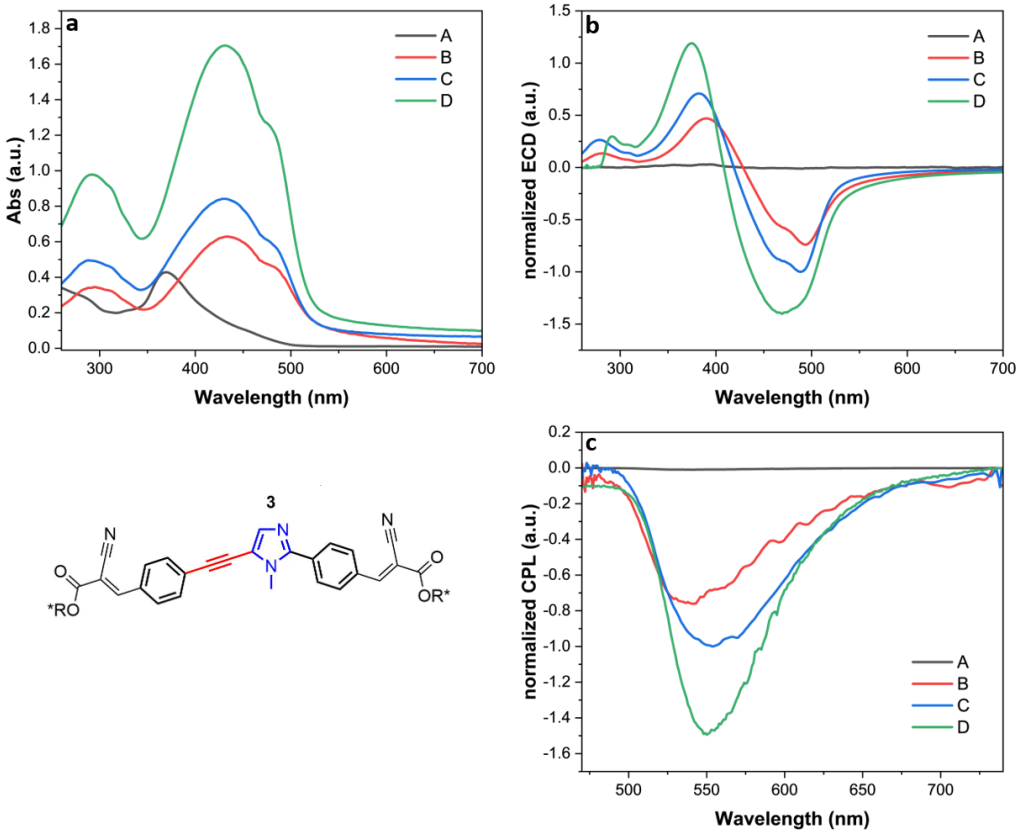

Fig. S7. (a) Absorption, (b) normalized ECD and (c) normalized CPL spectra of thin films of **3** with variable thickness (see above).

Microscopy

General information

Optical microscopy images and cross-polarized microscopy images were recorded with a Zeiss Discovery V8 microscope equipped with built-in linear polarizers.
Scanning electron microscopy images were acquired on a Zeiss 550 Crossbeam in FE-SEM mode using secondary electrons detection. Samples were coated with a 6 nm Pt layer.
AFM images were recorded with a Veeco Multimode, Instruments Inc. (USA), equipped with NanoScope IV controller. Images were obtained with RTESP tapping tips. Tip height 15-20 μm, front angle 15°, back angle 25°, side angle 17.5°, tip radius <10 nm, resonance frequency 250 kHz.

Circularly polarized microscopy (CPM) analysis for spatially resolved ECD mapping were performed with an instrumental setup we previously designed and tested.[S8]

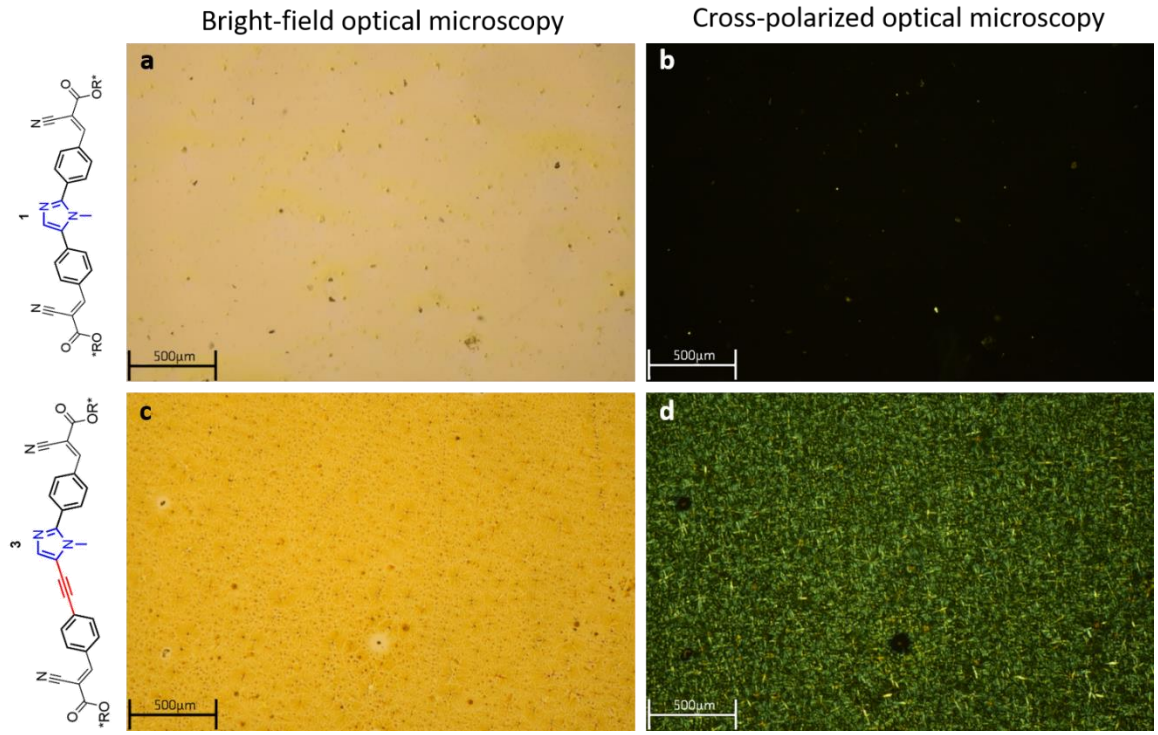

Fig. S8. (a) Bright-field optical microscopy and (b) cross-polarized microscopy images of compound **2** thin film. (c) Bright-field optical microscopy and (d) cross-polarized microscopy images of compound **4** thin film.

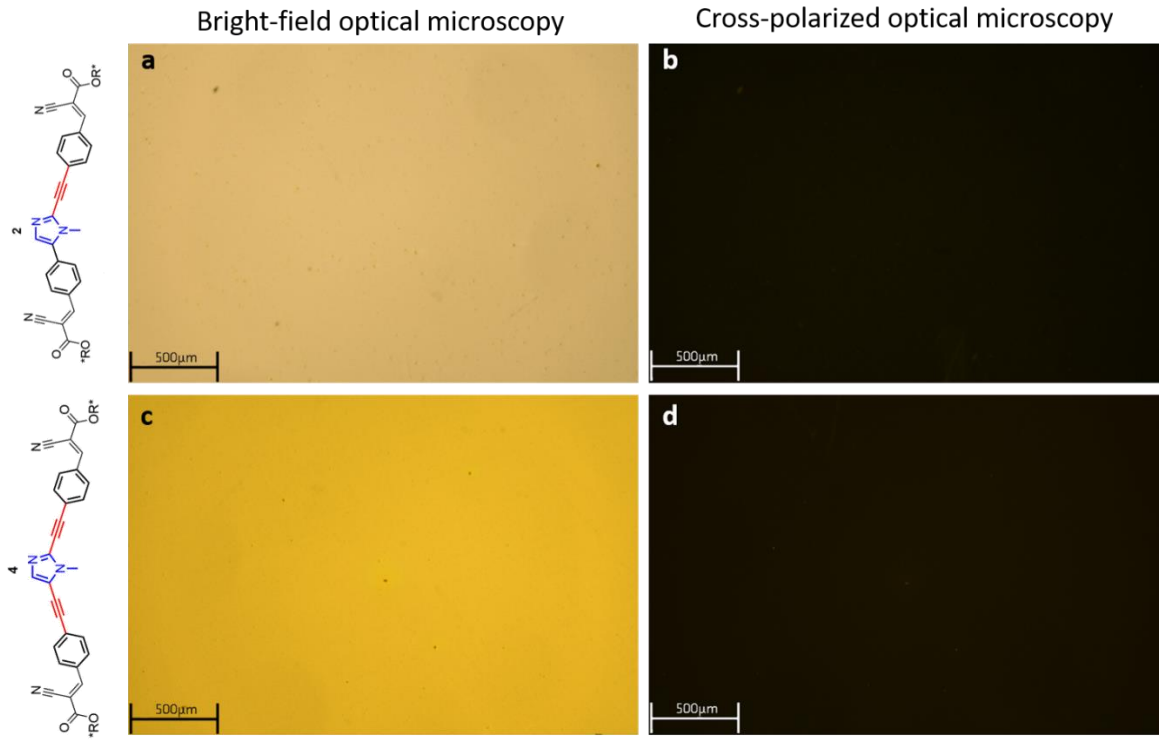

Fig. S9. (a) Bright-field optical microscopy and (b) cross-polarized microscopy images of compound **1** thin film. (c) Bright-field optical microscopy and (d) cross-polarized microscopy images of compound **3** thin film.

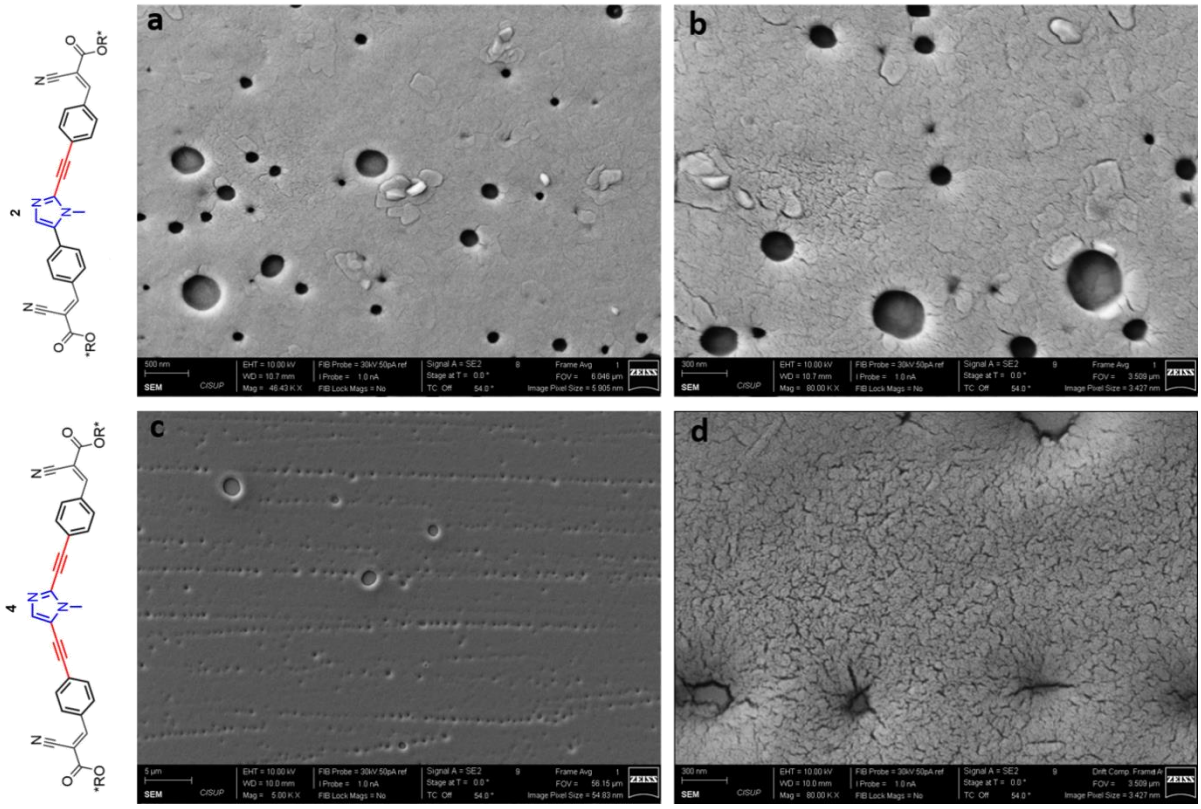

Fig. S10. (a,b) Scanning electron microscopy images of compound **2** thin film and (c,d) scanning electron microscopy images of compound **4** thin film.

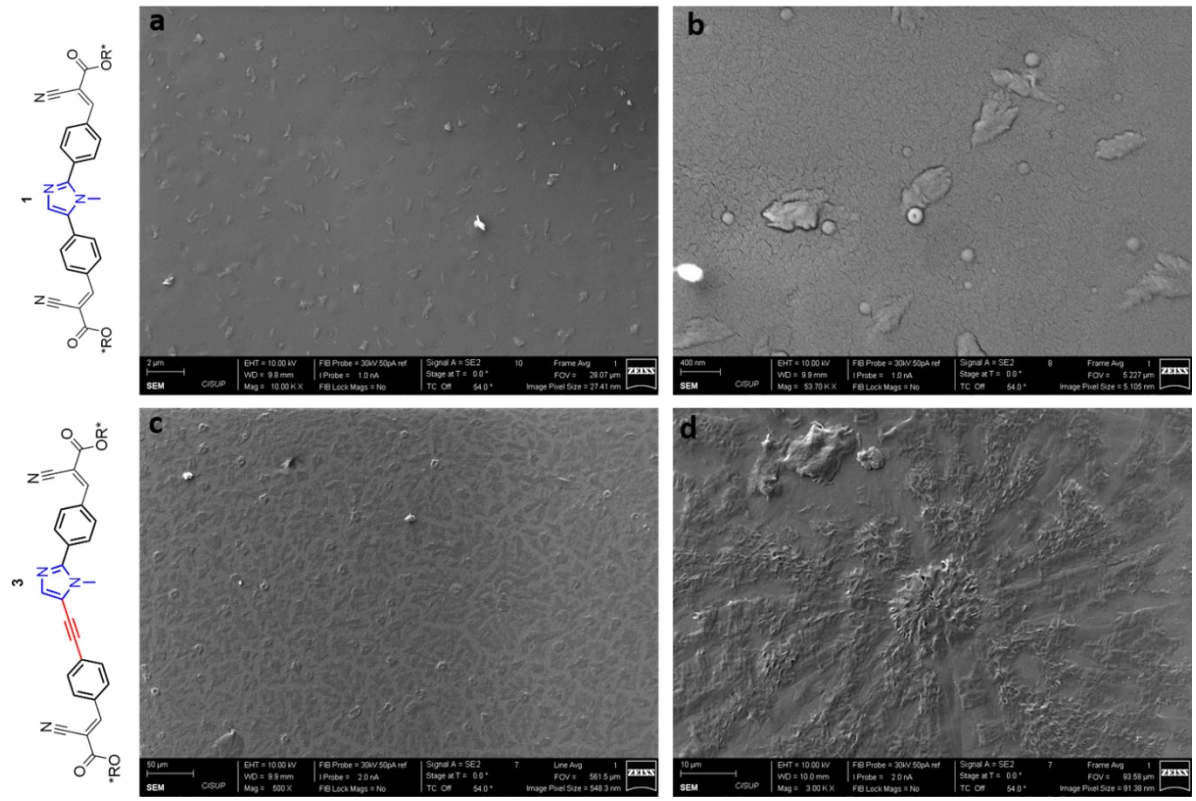

Fig. S11. (a,b) Scanning electron microscopy images of compound **1** thin film and (c,d) scanning electron microscopy images of compound **3** thin film.

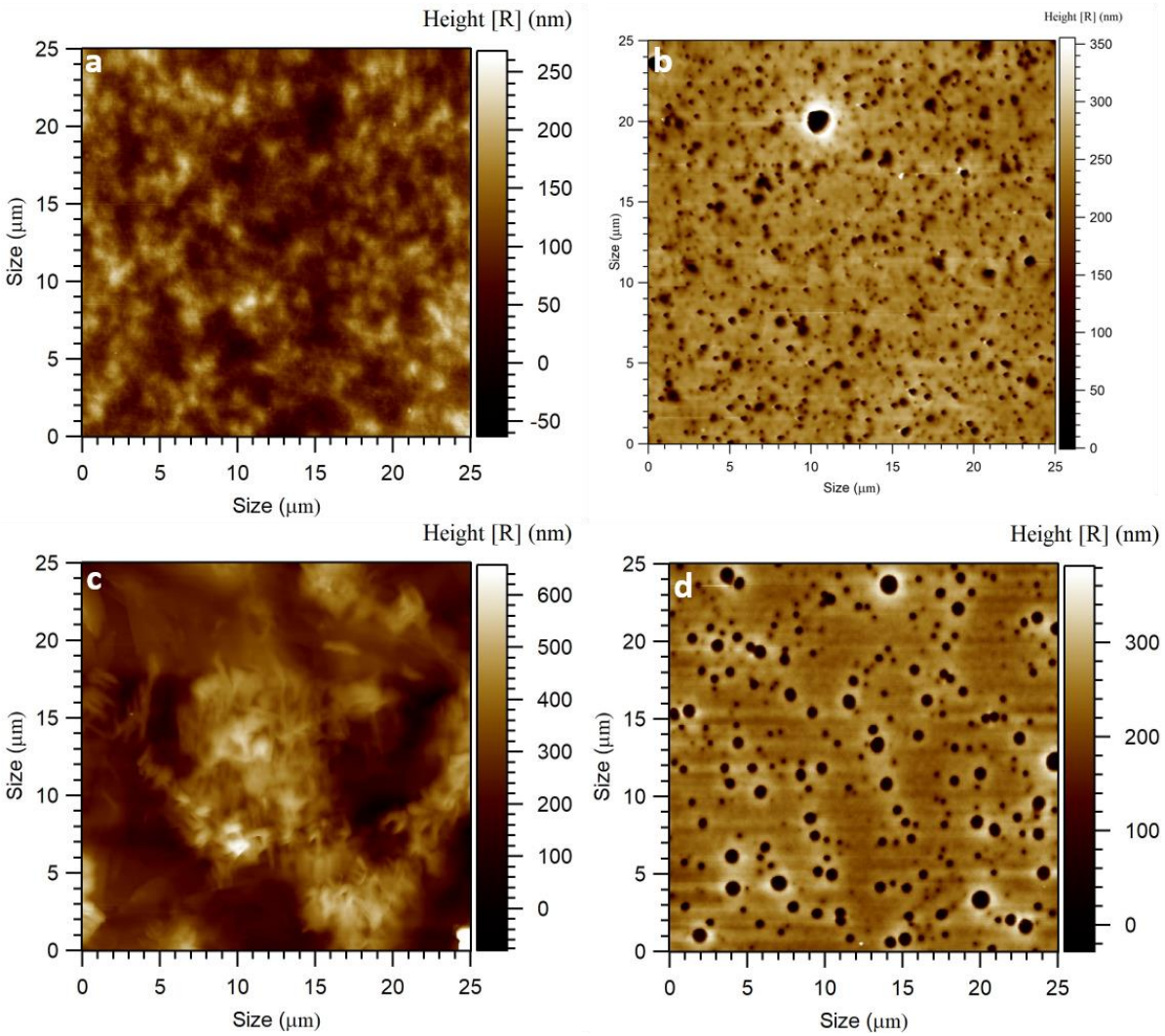

Fig. S12. AFM images of thin films made by (a) compound **1**, (b) compound **2**, (c) compound **3** and (d) compound **4**.

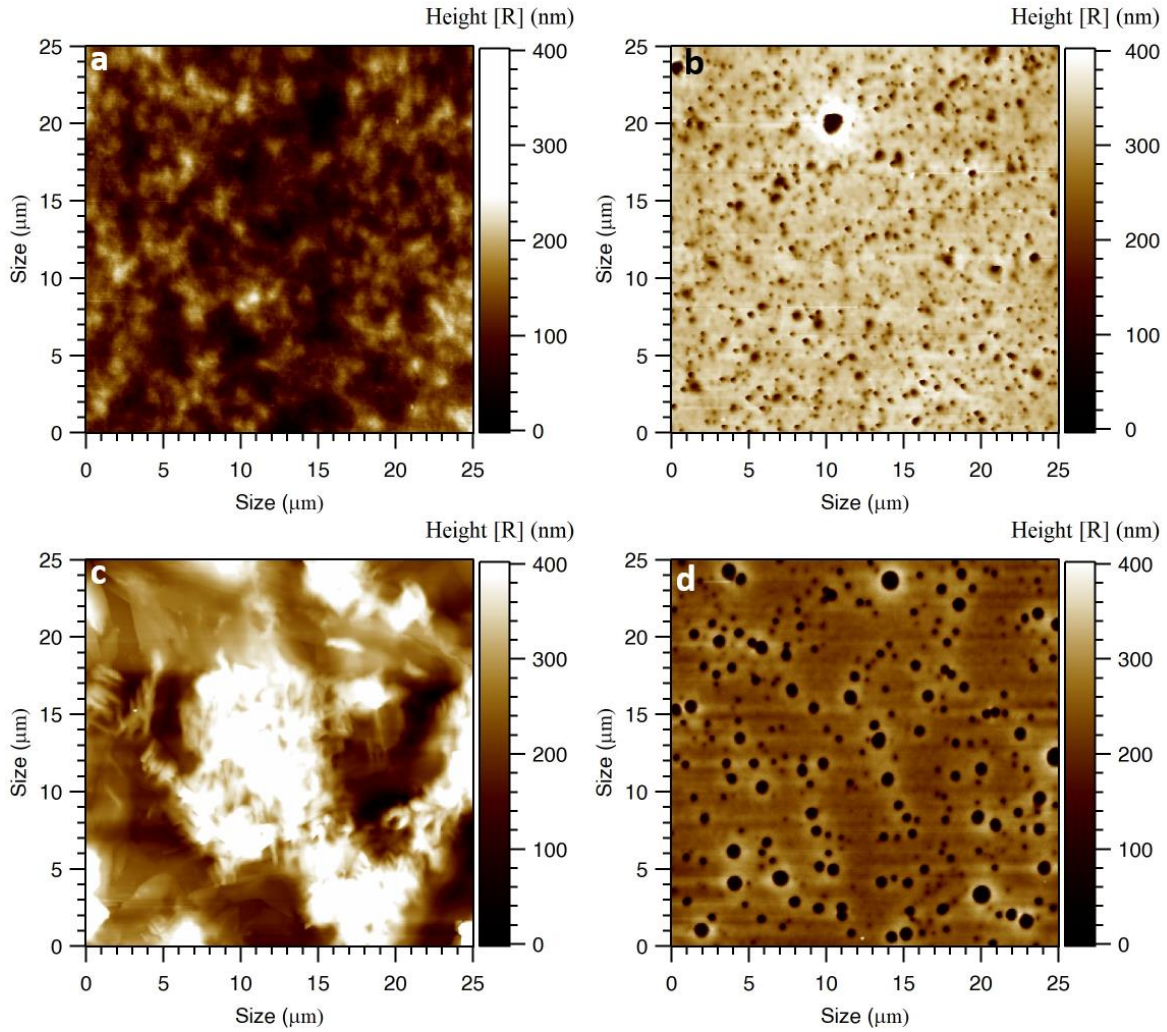

Fig. S13. AFM images of thin films made by (a) compound **1**, (b) compound **2**, (c) compound **3** and (d) compound **4** with the same scale of height (R).

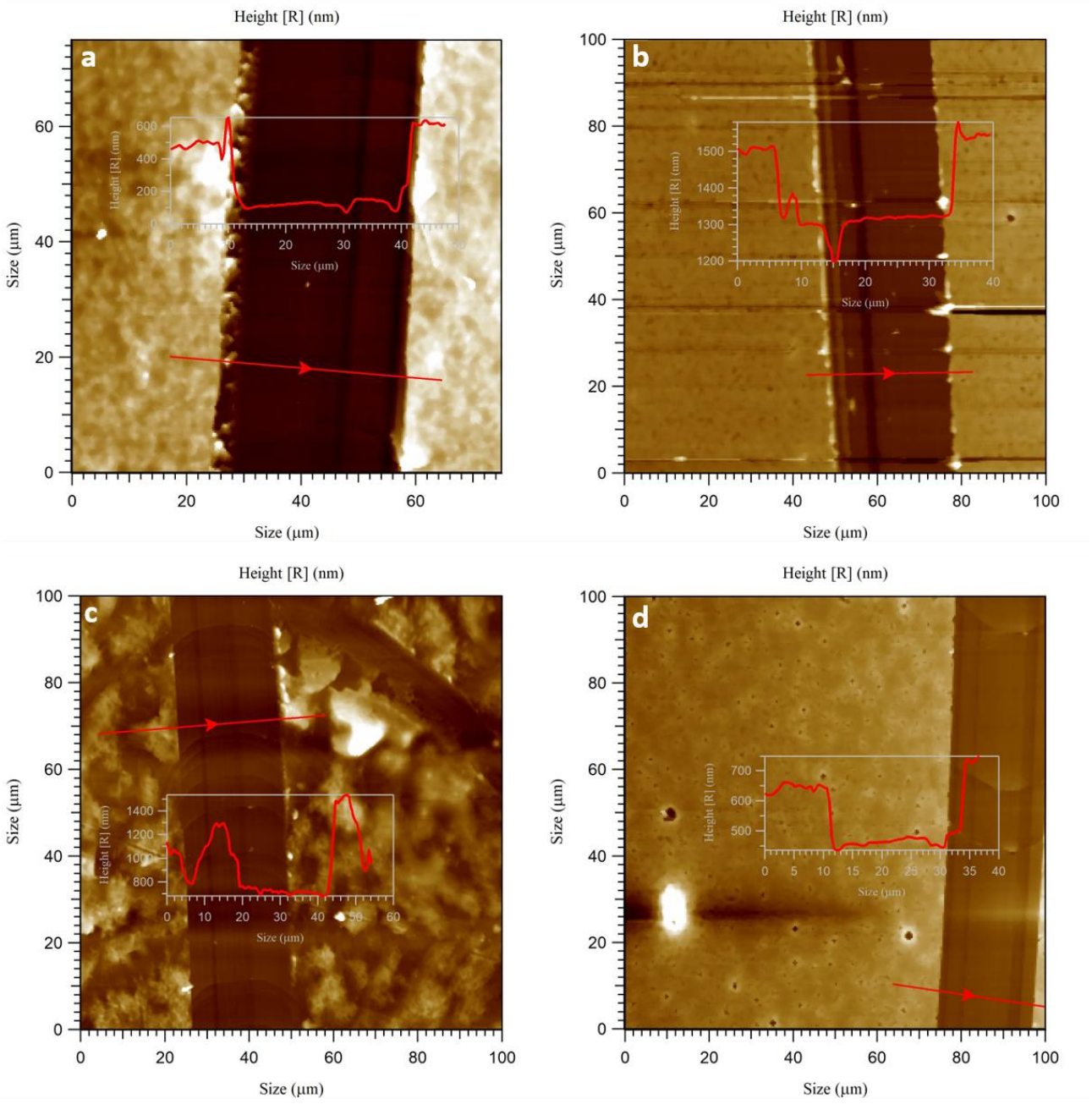

Fig. S14. Coarse film thickness estimation via monodimensional AFM projections of thin films made by (a) compound **1**, (b) compound **2**, (c) compound **3** and (d) compound **4**. The thicknesses were estimated through difference between the height of films and the height of the glass substrate.

Roughness

Roughness (RMS) was estimated as the RMS of the Z_i values from the AFM raster scans as:

$$RMS = \sqrt{\frac{1}{n}\sum_i Z_i^2}$$

With n the number of sampled points.

The following RMS were obtained:

Film of **1**: 36 nm

Film of **2**: 41 nm

Film of **3**: 99 nm

Film of **4**: 51 nm

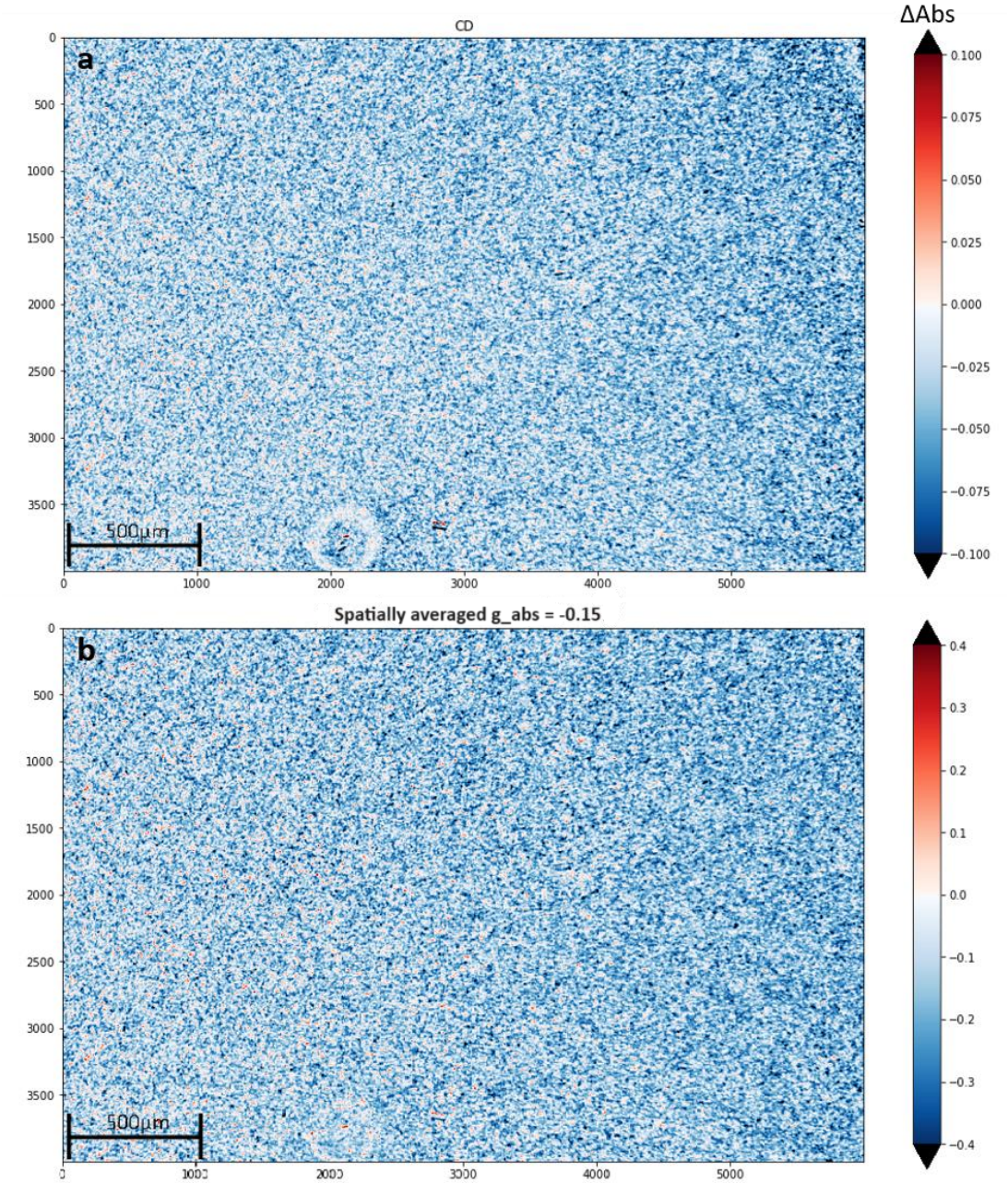

Fig. S15. CPM mapping of thin film made by compound **3**. (a) ECD map and (b) g_{abs} map. The analysis highlighted a predominant negative ECD activity, although with spatially different intensity, over all the surface studied. Bandpass filter: 500 nm (FWHM = 80 nm).

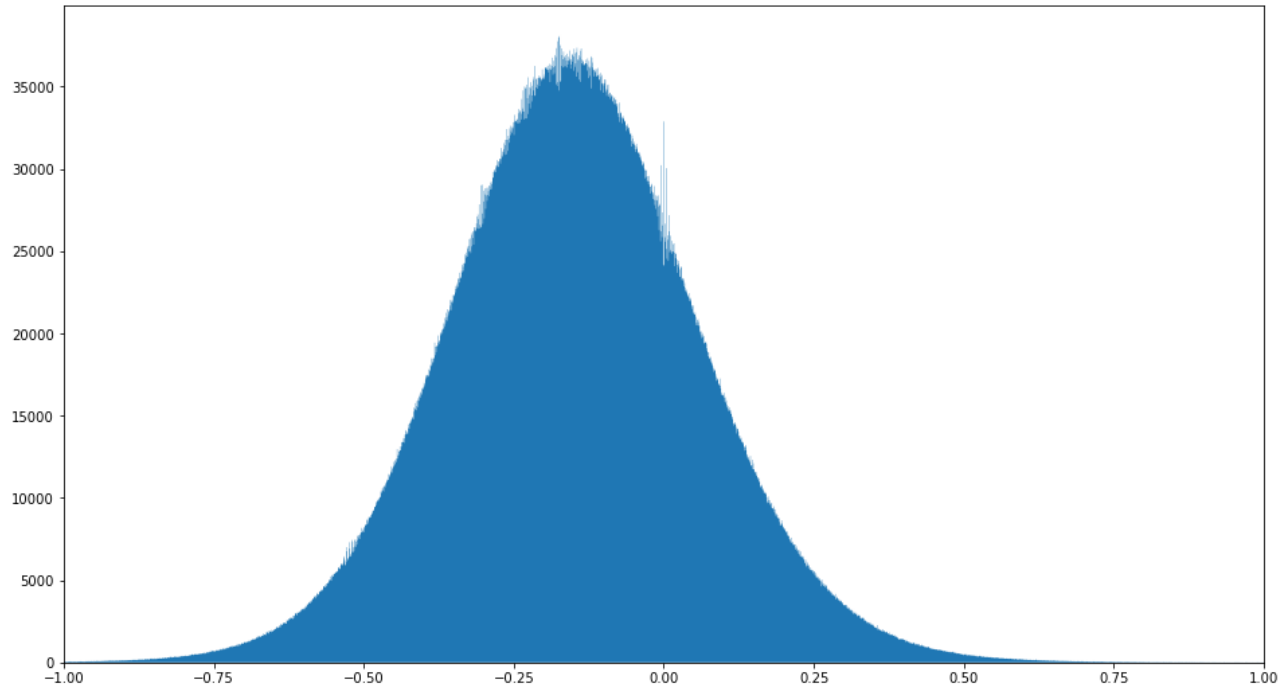

Fig. S16. Histogram representing the g_{abs} distribution in the CPM map.

Ultra-cheap CPL setup

General information

UV LED: 365 nm Thorlabs UV LED.
Circular polarizers: Edmund Optics polarizing polymer films CP42HE and CP42HER.
Bandpass filters: 600 nm and 650 nm Edmund Optics traditional coated filters (FWHM = 80 nm).
Photoresistor: 0-20 kOhm range. Commercially purchasable at less than 1 euro.
Ohmmeter: DM830E digital multimeter.

Total estimated cost: approximately 200 €.

When comparing the g_{lum} obtained with our ultra-cheap setup with the one obtained with our conventional CPL instrument, to formally compare data in a correct manner, we must consider the wavelength dependence of the components reported in **Fig. 2a**. In particular, the bandpass filters adopted are characterized by specific transmission spectra (**Fig. S14a** and **Fig. S14b**), moreover the photoresistor response is not constant at different wavelengths (**Fig. S14c**). Thus, we need to compare the two g_{lum} values obtained with the setup of **Fig. 2a** with two values extrapolated from the spectral g_{lum} by taking into account such wavelength dependences. This can be done through calculation of g_{lum} at 600 nm and 650 nm with ratios of integral means reported in **Eq. S1**. However, as reported in **Table S2**, the corrections on g_{lum} obtained are negligible, suggesting that wavelength dependences of bandpass filters and photoresistor response are not affecting the measurements, at least at these wavelengths.

Supporting data

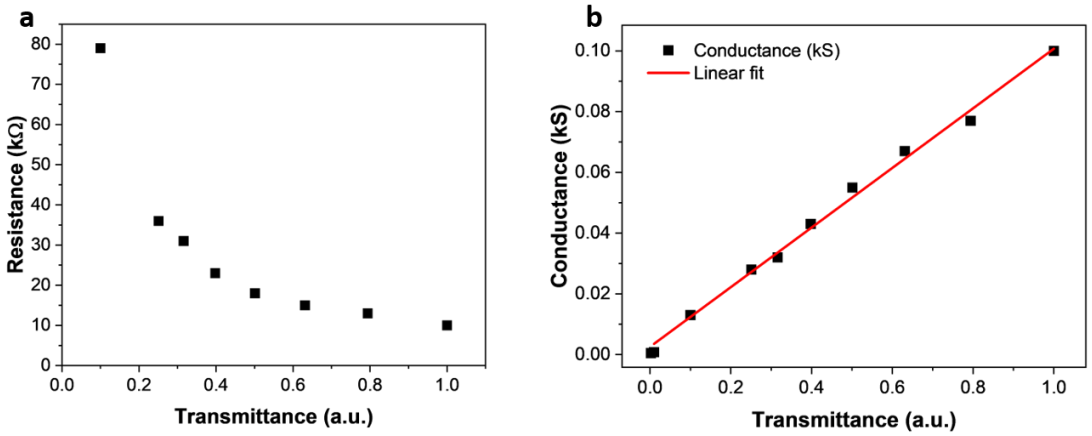

Fig. S17. Photoresistor response to the transmittance of filters with variable optical density at 470 nm expressed in (a) resistance and (b) conductance. The conductance showed a linear dependence with the transmission of light and, thus, the intensity of incident light.

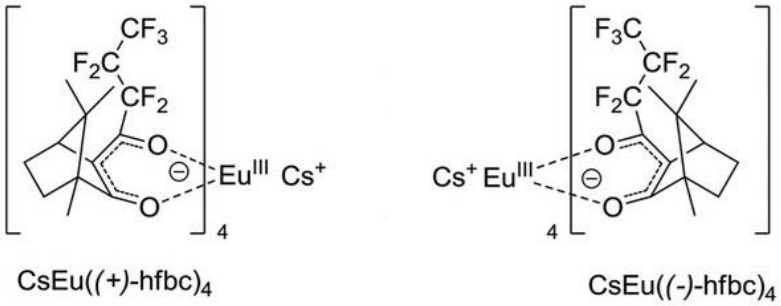

Fig. S18. Chemical structure of CsEu((+)hfbc)$_4$ and CsEu((-)hfbc)$_4$ complexes.

	g_{lum} mean value	**Standard deviation**
CsEu((+)hfbc)$_4$	1.298	0.011
CsEu((-)hfbc)$_4$	-1.300	0.010
Fluorescein	-0.009	0.007

Table S1. g_{lum} values and relative standard deviations obtained with our ultra-cheap CPL setup for CsEu(hfbc)$_4$ enantiomers solutions in $CHCl_3$ and for achiral fluorescein solution in ethanol over a set of 10 measurements for each sample.

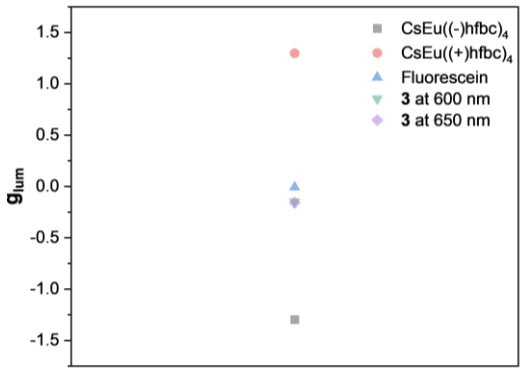

Fig. S19. Graphical representation of g_{lum} values and relative standard deviations obtained with our ultracheap CPL setup for $CsEu(hfbc)_4$ enantiomers solutions in $CHCl_3$, a fluorescein solution in ethanol over a set of 10 measurements for each sample and thin film of **3** (at 600 nm and 650 nm).

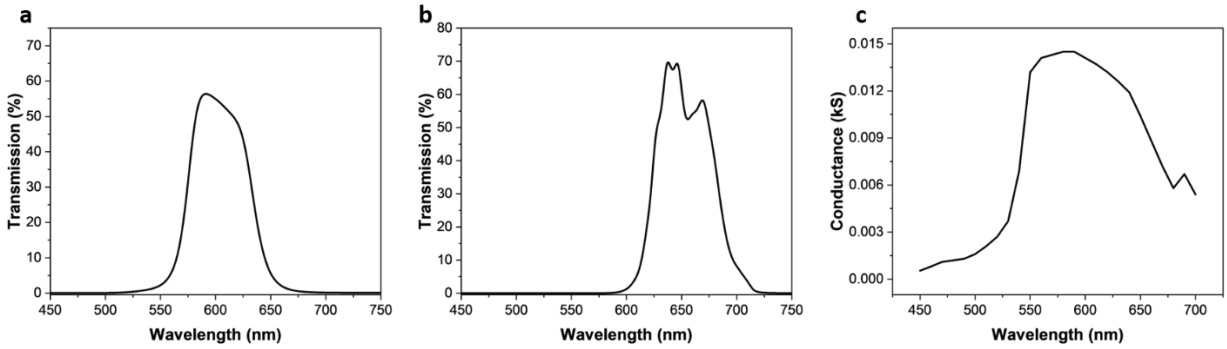

Fig. S20. Transmission spectra of bandpass filters centered at (a) 600 nm and (b) 650 nm. (c) Depiction of the photoresistor response (in conductance units) at different wavelengths.

$$g_{conv} = \frac{\int_{\lambda_-}^{\lambda_+} CPL(\lambda)\, T_{BP}(\lambda)\, G_{PR}(\lambda)\, d\lambda}{\int_{\lambda_-}^{\lambda_+} PL(\lambda)\, T_{BP}(\lambda)\, G_{PR}(\lambda)\, d\lambda} = \frac{\int_{\lambda_-}^{\lambda_+} CPL(\lambda)\, T_{BP}(\lambda)\, G_{PR}(\lambda)\, d\lambda}{\int_{\lambda_-}^{\lambda_+} PL(\lambda)\, T_{BP}(\lambda)\, G_{PR}(\lambda)\, d\lambda}$$

$$CPL: circularly\ polarized\ luminescence \qquad PL: photoluminescence\ (or\ total\ emission)$$

$$T_{BP}: bandpass\ filter\ transmission \qquad G_{PR}: wavelength\ dependence\ of\ the\ photoresistor\ response$$

Eq. S1. Equation involved in the convolution of g_{lum} value (g_{conv}) obtained from the standard CPL instrument to be compared with the g_{lum} obtained from the ultracheap CPL setup. All wavelength dependent contributions of the ultracheap CPL setup are taken into account in this equation. λ_- and λ_+ are, respectively, the minimum and the maximum wavelength of spectra.

	g_{conv}	g_{lum} from spectra
600 nm	-0.171	-0.174
650 nm	-0.131	-0.128

Table S2. g_{conv} values obtained from Eq. 1 in comparison with punctual g_{lum} spectral values obtained with the standard CPL instrument at 600 nm and 650 nm.

Computations

General information

The calculations were run on methyl ester analogues of compounds **1** and **3**, with the alkyl chains replaced by methyl groups. These model compounds are labelled trunc-**1** and trunc-**3**. Conformational searches and preliminary DFT calculations were run with Spartan'20 (Wavefunction, Irvine, CA, U.S.A.) with default parameters, default grids, and convergence criteria. Time-dependent DFT (TDDFT) calculations were run with Gaussian 16 (Revision C.01)[S9] with default grids and convergence criteria. The conformational search was run with the Monte Carlo algorithm implemented in Spartan'20 using MMFF (Merck molecular force field). All structures obtained thereof were optimized with DFT at the B3LYP-D3/6-31+G(d,p) level in vacuo. Several lo-energy minima were obtained: 26 conformers within 2 kcal/mol for trunc-**1** and 14 conformers within 2 kcal/mol for trunc-**3**. The two lowest-energy conformers with the –CN groups pointing in the same direction (named *syn*) and opposite direction (named *anti*) for each compound were considered for further analysis. TD-DFT calculations were run with the B3LYP and CAM-B3LYP functionals and def2-TZVP basis set. Only CAM-B3LYP results are discussed below. Natural transition orbitals (NTO) were plotted with MultiWfn v3.81.[S10]
UV and ECD spectra were plotted using the program SpecDis (version 1.71, Berlin: Germany, http://specdis-software.jimdo.com), with exponential bandwidth σ=0.4-0.5 eV.

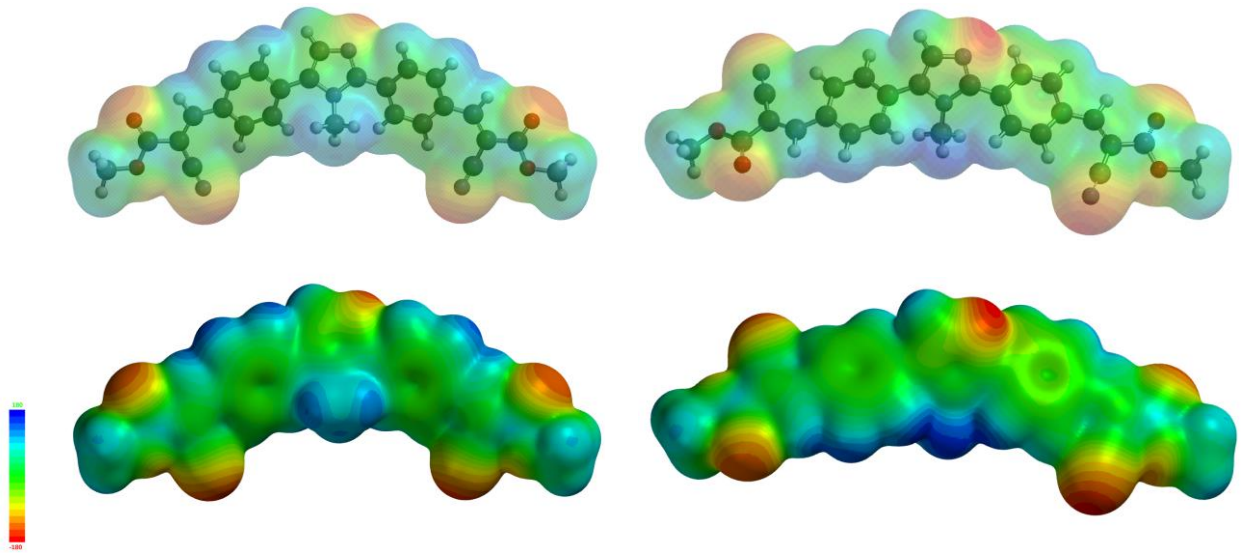

Syn conformer (abs. min) *Anti* conformer (+0.1 kcal/mol)

Fig. S21. Lowest-energy DFT structures of compound trunc-**1** and potential energy surfaces (isovalue 0.002 e/au^3, boundary -180/180 kJ). The plots suggest that the major aggregation mode may involve side-to-side interactions rather than face-to-face ones.

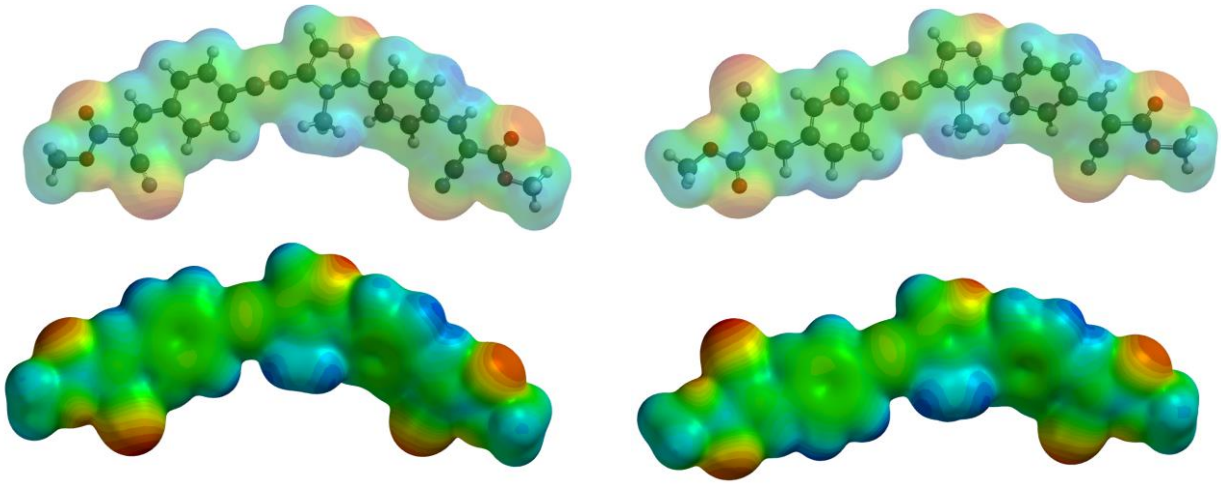

Syn conformer (abs. min) *Anti* conformer (+0.1 kcal/mol)

Fig. S22. Lowest-energy DFT structures of compound trunc-**3** and potential energy surfaces (isovalue 0.002 e/au^3, boundary -180/180 kJ).

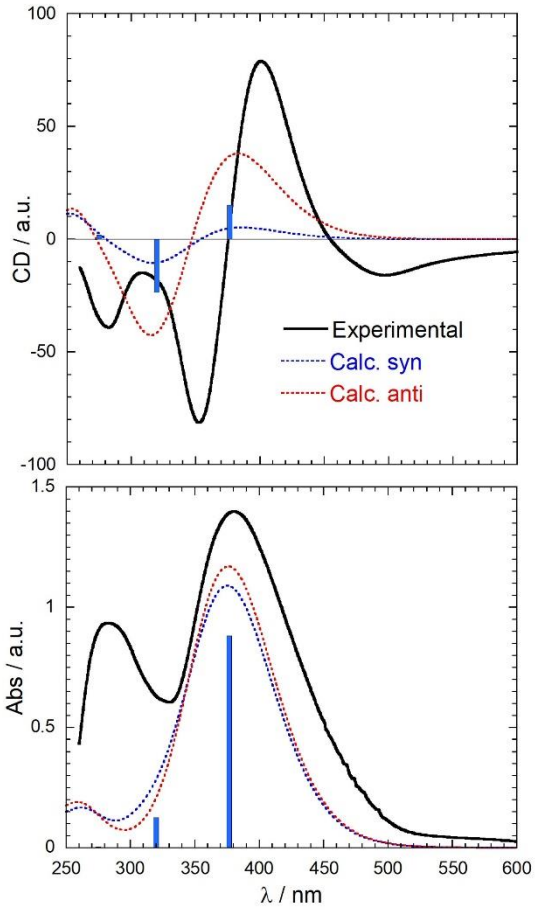

Fig. S23. Experimental thin-film UV and ECD spectra of **1** compared with TD-DFT calculated spectra of trunc-**1**. The calculated ECD signals are due to the chiral conformations of trunc-**1** used in the calculations. Placing the first calculated UV band in correspondence with the experimental maximum (and the couplet crossover), the second calculated transition lies afar from the high-energy couplet branch.

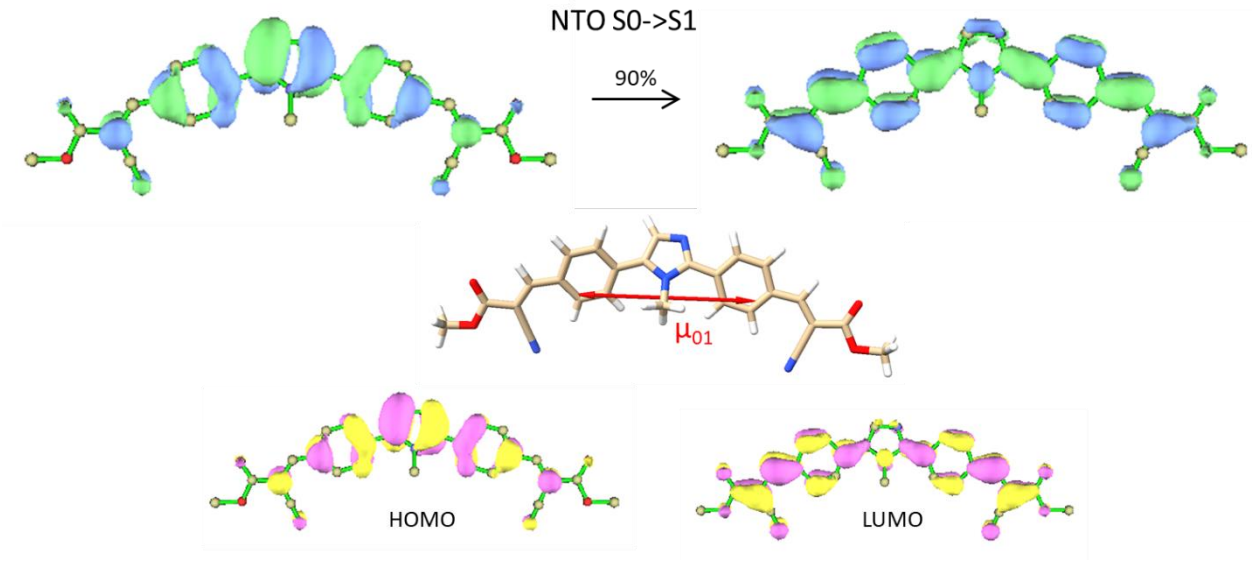

Fig. S24. Natural transition orbitals, electric transition dipole and frontier orbitals calculated with TD-DFT for the first transition of trunc-**1** (*syn* geometry). The S0-S1 transition can be described as a centre-to-periphery charge transfer, dominated by the HOMO-LUMO excitation. The electric transition dipole is roughly parallel to the major axis.

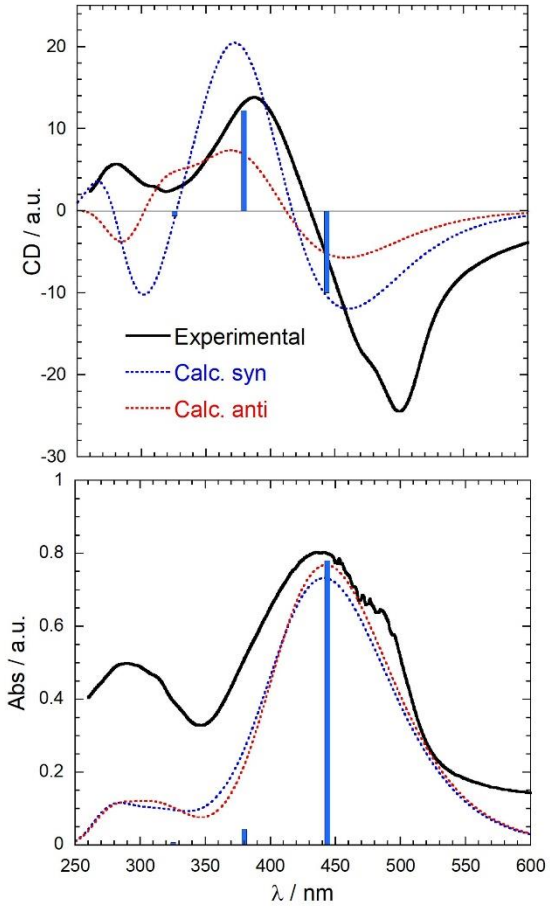

Fig. S25. Experimental thin-film UV and ECD spectra of **3** compared with TD-DFT calculated spectra of trunc-**3**. The calculated ECD signals are due to the chiral conformations of trunc-**3** used in the calculations. Placing the first calculated UV band in correspondence with the experimental maximum, the second calculated transition matches the second experimental ECD band.

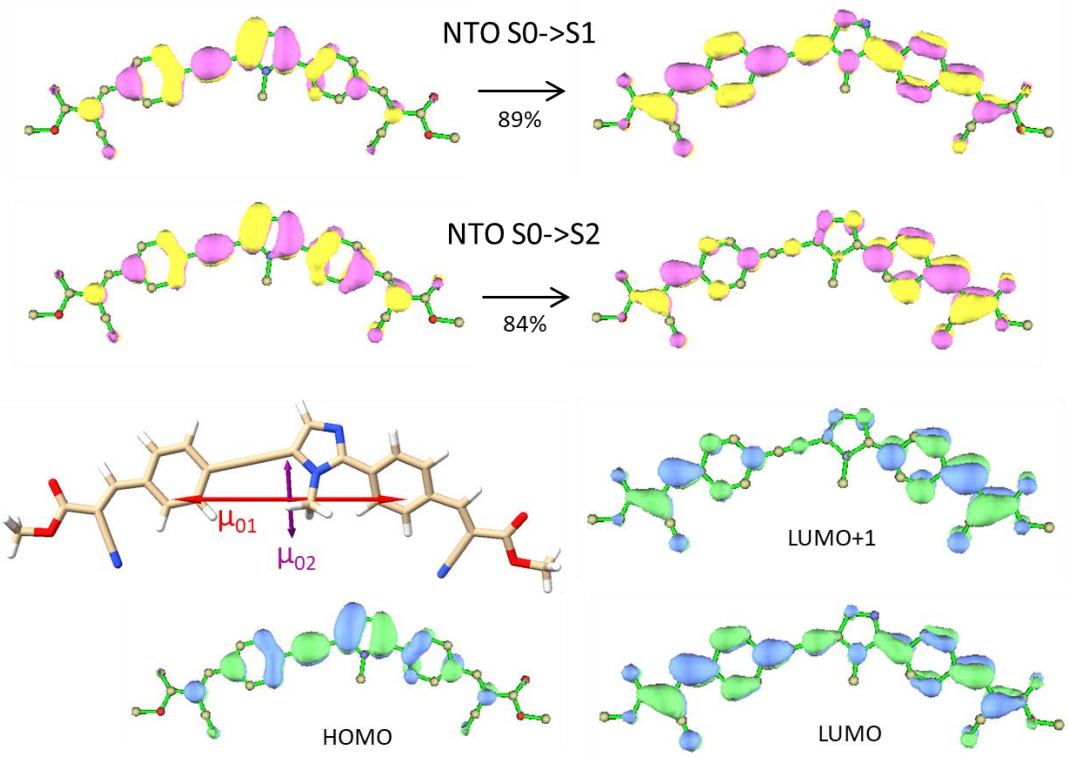

Fig. S26. Natural transition orbitals, electric transition dipoles and frontier orbitals calculated with TD-DFT for the first two transitions of trunc-**3** (*syn* geometry). The S0-S1 transition can be described as a charge transfer toward the phenylethynyl side, dominated by the HOMO-LUMO excitation; the S0-S2 as a charge transfer toward the opposite side, dominated by the HOMO-LUMO+1 excitation. The two electric transition dipoles are roughly orthogonal to each other.

References

S1 A. Takfaoui, L. Zhao, R. Touzani, J.-F. Soulé, P. H. Dixneuf, H. Doucet, *Tetrahedron*, 2014, **70**, 8316–8323.

S2 R. Bhaskar, A. K. Sharma, A. K. Singh, *Organometallics*, 2018, **37**, 2669–2681.

S3 G. Del Frate, F. Bellina, G. Mancini, G. Marianetti, P. Minei, A. Pucci, V. Barone, *Phys. Chem. Chem. Phys.*, 2016, **18**, 9724–9733.

S4 K. G. Holden, M. N. Mattson, K. H. Cha, H. Rapoport, *J. Org. Chem.*, 2002, **67**, 5913–5918.

S5 F. Zinna, T. Bruhn, C. A. Guido, J. Ahrens, M. Bröring, L. Di Bari, G. Pescitelli, *Chem. Eur. J.*, 2016, **22**, 16089–16098.

S6 F. Zinna, G. Albano, A. Taddeucci, T. Colli, L. A. Aronica, G. Pescitelli, L. Di Bari, *Adv. Mater.*, 2020, **32**, 2002575.

S7 G. Albano, G. Pescitelli and L. Di Bari, *Chem. Rev.*, 2020, **120**, 10145–10243.

S8 A. Taddeucci, F. Zinna, G. Siligardi, L. Di Bari, *Chem. Biomed. Imaging*, 2023, **1**, 471–478.

S9 M. J. Frisch, G. W. Trucks, H. B. Schlegel, G. E. Scuseria, M. A. Robb, J. R. Cheeseman, G. Scalmani, V. Barone, G. A. Petersson, H. Nakatsuji, X. Li, M. Caricato, A. V. Marenich, J. Bloino, B. G. Janesko, R. Gomperts, B. Mennucci, H. P. Hratchian, J. V. Ortiz, A. F. Izmaylov, J. L. Sonnenberg, D. Williams-Young, F. Ding, F. Lipparini, F. Egidi, J. Goings, B. Peng, A. Petrone, T. Henderson, D. Ranasinghe, V. G. Zakrzewski, J. Gao, N. Rega, G. Zheng, W. Liang, M. Hada, M. Ehara, K. Toyota, R. Fukuda, J. Hasegawa, M. Ishida, T. Nakajima, Y. Honda, O. Kitao, H. Nakai, T. Vreven, K. Throssell, J. A. Montgomery, Jr., J. E. Peralta, F. Ogliaro, M. J. Bearpark, J. J. Heyd, E. N. Brothers, K. N. Kudin, V. N. Staroverov, T. A. Keith, R. Kobayashi, J. Normand, K. Raghavachari, A. P. Rendell, J. C. Burant, S. S. Iyengar, J. Tomasi, M. Cossi, J. M. Millam, M. Klene, C. Adamo, R. Cammi, J. W. Ochterski, R. L. Martin, K. Morokuma, O. Farkas, J. B. Foresman, and D. J. Fox, Gaussian, Inc., Wallingford CT, 2016.

S10 T. Lu, F. Chen, *J. Comput. Chem.*, 2012, **33**, 580–592.